the positions for the different models were insignificant, and in all cases the coordinates derived from Guinier data agreed with the corresponding single-crystal results within the e.s.d.'s. The lower precision of the coordinates derived from Guinier data is primarily a consequence of the limited region of reciprocal space which is sampled, $\sin\theta/\lambda < 0{\cdot}46$ Å^{-1}: the precision of the data itself is comparable with that of the single-crystal data. Temperature factors correlate highly with the absorption corrections and cannot be determined meaningfully from Guinier data: however, the results suggest that the differences between atomic temperature factors may be physically significant, albeit with rather low accuracy.

The absorption correction calculated for a uniform specimen proved a poor approximation, doing little if anything to reduce either R_w or the magnitude of the overall temperature factor (which is considered to be a measure of uncorrected systematic errors) for the structures refined. In one case, yttrium oxide, the absorption correction with an empirically optimized coefficient did significantly reduce R_w and the e.s.d.'s of the parameters: however, the magnitude of the overall temperature factor increased greatly and the optimized absorption coefficient was more than five times the calculated average value, so that the physical significance of this correction is uncertain.

In practice, it appears possible in many cases to correct effectively for systematic errors, including specimen absorption, by a single overall temperature factor (which may be either positive or negative) as proposed by Werner *et al.* (1979). Good agreement between the model and the data was obtained in this way for the three structures studied here. However, in some cases an improved fit, and hence more precise parameter estimates, may be achieved by including a correction of the form given by Sas & de Wolff (1966) for specimen absorption. Both these corrections are of an *ad hoc* nature, and are not to be considered as the direct physical consequence of thermal or absorption effects.

References

International Tables for X-ray Crystallography (1974). Vol. IV. Birmingham: Kynoch Press.

MALMROS, G. & THOMAS, J. O. (1977). *J. Appl. Cryst.* **10**, 7–11.

PATON, M. G. & MASLEN, E. N. (1965). *Acta Cryst.* **19**, 307–310.

RIETVELD, H. M. (1967). *Acta Cryst.* **22**, 151–152.

RIETVELD, H. M. (1969). *J. Appl. Cryst.* **2**, 65–71.

ROSSELL, H. J. & SCOTT, H. G. (1975). *J. Solid State Chem.* **13**, 345–350.

SAKATA, M. & COOPER, M. J. (1979). *J. Appl. Cryst.* **12**, 554–563.

SAS, W. H. & DE WOLFF, P. M. (1966). *Acta Cryst.* **21**, 826–827.

SMITH, G. S. & ISAACS, P. B. (1964). *Acta Cryst.* **17**, 842–846.

WERNER, P.-E. (1971). *J. Phys. E*, **4**, 351–353.

WERNER, P.-E., MARINDER, B.-O. & MAGNÉLI, A. (1978). *Mater. Res. Bull.* **13**, 1371–1378.

WERNER, P.-E., SALOMÉ, S., MALMROS, G. & THOMAS, J. O. (1979). *J. Appl. Cryst.* **12**, 107–109.

WILLIAMS, R. J., DILLIN, D. R. & MILLIGAN, W. O. (1973). *Acta Cryst.* B**29**, 1369–1372.

Acta Cryst. (1981). A**37**, 459–465

Multiple Bragg Reflections of Neutrons in an Elastically Deformed Single Crystal

BY M. VRÁNA, P. MIKULA, R. T. MICHALEC, J. KULDA AND J. VÁVRA

Nuclear Physics Institute of the Czechoslovak Academy of Sciences, 250 68 Řež near Prague, Czechoslovakia

(*Received* 26 *February* 1980; *accepted* 3 *November* 1980)

Abstract

The large positive diffraction intensity changes on forbidden (222) planes, which are produced by simultaneous diffraction, were observed when a perfect Si single crystal was excited into vibration. The excited *Umweganregung* effect is of the same order as the diffraction intensity obtained on (111) planes under the same experimental conditions. The theoretical consideration is an extension of the lamellae model usually used in the two-wave approximation. Both the theory and the experimental results demonstrate that such an effect may cause very large errors especially in diffraction experiments with non-perfect single crystals.

0567-7394/81/040459-07$01.00

© 1981 International Union of Crystallography

1. Introduction

Since the first experiment performed with X-rays by Renninger (1937), simultaneous reflection has been quantitatively studied by a number of authors and its effect on intensity data in the case of perfect crystals is well known. Besides the negative role that the presence of the simultaneous reflection may play in accurate measurements of a primary reflection intensity from single crystals, the observation of the enhancement of the anomalous transmission in the many-beam region angles (Bormann & Hartwig, 1965) has meant that the interest in simultaneous X-ray diffraction has continuously increased.

Simultaneous Bragg reflections of neutrons in mosaic crystals were studied by Moon & Shull (1964). These authors also developed an approximative theory of simultaneous reflections based on the mosaic-crystal model. Thompson & Grimes (1977) experimentally showed that neutron diffraction appears to have inherent difficulties and severe limitations resulting from the presence of simultaneous reflections when a mosaic single crystal whose space group has to be determined through the examination of very weak reflections is used.

As the flux of thermal neutrons is usually not sufficiently high, the observation of such small effects with neutrons on perfect crystals is very difficult. A simple estimation shows that the intensity corresponding to the simultaneous reflection is in relation to the primary reflection intensity as the width of the dynamical maximum to the angular divergence of the incident beam.

In our previous paper – hereafter referred to as paper I (Mikula, Vrána, Michalec & Vávra, 1979), we first gave a simple scheme to show how the intensity diffracted due to the *Umweg* effect can be made clearly observable with an elastically deformed perfect crystal. In the case of silicon (diamond structure), this effect occurs for those forbidden reflections with even indices only (*e.g.* 222); the multiple reflections operative in these cases may then be of the odd–odd type only. In our first experiment with the neutron wavelength $\lambda = 1{\cdot}05 \times 10^{-1}$ nm, we observed many excited *Umweg* peaks which were much more intense than the second-order reflection. For such a short wavelength, the *Umweg* peaks are very dense and can hardly be resolved experimentally.

The purpose of this paper is to carry out a more extensive investigation (both theoretically and experimentally) of the observed *Umweg* effect for $\lambda = 1{\cdot}54 \times 10^{-1}$ nm, where the density of the *Umweg* peaks is much lower than for $\lambda = 1{\cdot}05 \times 10^{-1}$ nm. The measured intensities are interpreted in terms of the lamellae model (Michalec, Chalupa, Sedláková, Mikula, Petržílka & Zelenka, 1974), according to which the diffracted intensity is proportional to the variation of the actual Bragg angle along the diffracted beam path in the deformed crystal instead of the structure factor. Clearly, for high deformations, this proportionality becomes saturated as soon as the intensity approaches the value predicted by the kinematical theory.

2. Theoretical consideration

Let us suppose that a beam of neutrons represented by the wave vector $\mathbf{k}_0$ impinges on a surface of a perfect nonabsorbing single crystal at the exact setting for simultaneous three-beam diffraction (see Fig. 1). The conditions for simultaneous reflection on two systems of planes 1 and 2 represented by their reciprocal-lattice vectors $\mathbf{g}_1$ and $\mathbf{g}_2$ can be expressed in the form

$$\mathbf{k}_0 \cdot \mathbf{g}_1 = -\mathbf{g}_1^2/2 \qquad (1a)$$

$$\mathbf{k}_0 \cdot \mathbf{g}_2 = -\mathbf{g}_2^2/2. \qquad (1b)$$

If the reflection 1 is forbidden (structure factor $F_1 = 0$), it is known that a non-zero intensity can be observed in the direction of the primary reflection, $(\mathbf{k}_0 + \mathbf{g}_1)/|\mathbf{k}_0|$, as a result of a cooperative action of two allowed reflections 2 and 3 (secondary and tertiary). It follows from (1*a*) and (1*b*) that, for a beam of neutrons reflected on a system of planes 2, the Bragg condition is simultaneously fulfilled on a system of planes 3 represented by its reciprocal-lattice vector $\mathbf{g}_3 = \mathbf{g}_1 - \mathbf{g}_2$ (the Bragg angles corresponding to the systems 1, 2 and 3 we denote θ_1, θ_2 and θ_3, respectively).

$$(\mathbf{k}_0 + \mathbf{g}_2) \cdot (\mathbf{g}_1 - \mathbf{g}_2) = -(\mathbf{g}_1 - \mathbf{g}_2)^2/2. \qquad (2)$$

The wave vectors $\mathbf{k}_0$ fulfilling (1*a*) and (1*b*) form a line in the reciprocal space. Only that part of the line which is restricted by the angular collimation of an incident beam participates in simultaneous diffraction.

It follows from the dynamical theory that, together with the neutrons exactly fulfilling (1*a*) and (1*b*), the

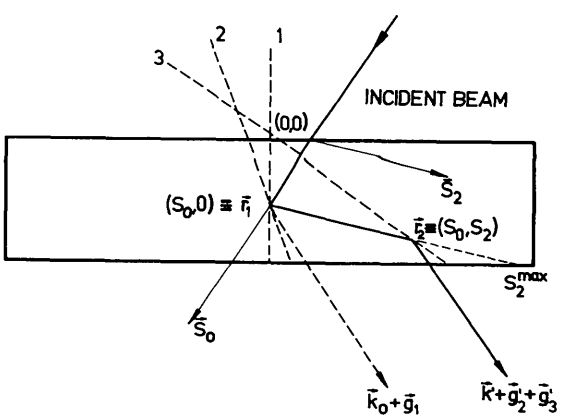

Fig. 1. Schematic diagram of multiple Bragg reflection simulating a weak or forbidden reflection.

neutrons having the wave vector $\mathbf{k} = \mathbf{k}_0 + \Delta\mathbf{k}_D$ also participate in simultaneous diffraction, where $\Delta\mathbf{k}_D$ is defined by the width of the dynamical maximum (Azároff, Kaplow, Kato, Weiss, Wilson & Young, 1974). The region of the wave vectors taking part in simultaneous diffraction is much smaller than the region corresponding to an allowed diffraction on a single system of planes, because in the three-wave case both the conditions (1*a*) and (1*b*) must be fulfilled, while in the two-wave case fulfilling (1*a*) is sufficient. A simple estimation shows that the diffraction intensities corresponding to the three- and two-wave cases are at the ratio of the width of the dynamical maximum to the angular collimation of the incident beam. So, in the case of perfect crystals, the observation of this small effect is very difficult.

The region of the wave vectors $\mathbf{k}$ participating in simultaneous diffraction may be substantially enlarged if the single crystal is elastically deformed. It is known from the two-wave approximation that the reflected intensity from a sufficiently thick elastically deformed crystal (when the crystal thickness is many times higher than the extinction length) is proportional to the total change of the Bragg angle along the path of the incident neutrons through the crystal (Buras, Giebułtowicz, Minor & Rajca, 1972). Usually, this proportionality, which enables the application of the lamellae model, can be observed in the wide scale of deformation.

The lamellae model is also applicable in our three-wave case if we suppose that the most important role in the multiple diffraction process is played by neutrons successively and independently reflected on the system of planes 2 and 3 during their path through the crystal (see Fig. 1). It means that we take into account only the neutrons doubly reflected at two different points with generally different deformation. Further, we suppose that the mutual distance of these points is larger than the extinction length.

Let $\mathbf{u}(\mathbf{r})$ be the displacement representing the deformation of a crystal at a point $\mathbf{r}$, $\mathbf{k}$ the wave vector fulfilling conditions (1*a*) and (1*b*) and $\mathbf{k}' = \mathbf{k} + \Delta\mathbf{k}$ is the wave vector of an incident neutron. The vectors of the local reciprocal lattice of a slightly deformed crystal are given by the relation (Takagi, 1969)

$$\mathbf{g}_2'(\mathbf{r}) = \mathbf{g}_2 - \nabla(\mathbf{g}_2.\mathbf{u}(\mathbf{r})). \tag{3}$$

Similarly,

$$\mathbf{g}_3'(\mathbf{r}) = (\mathbf{g}_1 - \mathbf{g}_2) - \nabla[(\mathbf{g}_1 - \mathbf{g}_2).\mathbf{u}(\mathbf{r})]. \tag{4}$$

If an incident neutron of $\mathbf{k}'$ is reflected at a point $\mathbf{r}_1 = (\mathbf{k}_0/|\mathbf{k}_0|)s_0$ on the path through the crystal, its Bragg condition is of the following form:

$$\mathbf{k}'(\mathbf{r}_1).\mathbf{g}_2'(\mathbf{r}_1) = -[\mathbf{g}_2'(\mathbf{r}_1)]^2/2. \tag{5}$$

This neutron, with wave vector $\mathbf{k}'(\mathbf{r}_1) + \mathbf{g}_2'(\mathbf{r}_1)$, can be once more reflected on the system of planes 3 if, on its path through the crystal, at a point

$$\mathbf{r}_2 = \mathbf{r}_1 + \frac{\mathbf{k}'(\mathbf{r}_1) + \mathbf{g}_2'(\mathbf{r}_1)}{|\mathbf{k}'|} s_2 = \mathbf{r}_1 + \mathbf{s}_2, \tag{6}$$

the local Bragg condition

$$(\mathbf{k}'(\mathbf{r}_1) + \mathbf{g}_2'(\mathbf{r}_1)).(\mathbf{g}_1'(\mathbf{r}_2) - \mathbf{g}_2'(\mathbf{r}_2)) = -[\mathbf{g}_1'(\mathbf{r}_2) - \mathbf{g}_2'(\mathbf{r}_2)]^2/2 \tag{7}$$

is fulfilled. As $\mathbf{u}(\mathbf{r}_1) \neq \mathbf{u}(\mathbf{r}_2)$ generally, the wave vector of the above-mentioned neutron does not suit the relationship

$$\mathbf{k}'(\mathbf{r}_1).\mathbf{g}_1'(\mathbf{r}_1) = -(\mathbf{g}_1'(\mathbf{r}_1))^2/2. \tag{8}$$

The quantities $\nabla(\mathbf{g}_2.\mathbf{u}(\mathbf{r}_1))$ and $\nabla[(\mathbf{g}_1 - \mathbf{g}_2).\mathbf{u}(\mathbf{r}_2)]$ are very small in comparison to $\mathbf{g}_2$ and $(\mathbf{g}_1 - \mathbf{g}_2)$, respectively. So the deviation of the doubly reflected neutron from the $(\mathbf{k}_0 + \mathbf{g}_1)/|\mathbf{k}_0|$ direction is negligible. Neglecting the corrections of second order, we obtain from (1), (3) and (7)

$$\begin{aligned}(\Delta\mathbf{k}.\mathbf{g}_2) &= |\mathbf{k}| \left.\frac{\partial(\mathbf{g}_2.\mathbf{u})}{\partial s_2}\right|_{\mathbf{r}_1} \equiv A(s_0),\\ (\Delta\mathbf{k}.\mathbf{g}_1) &= |\mathbf{k}| \left[\left.\frac{\partial(\mathbf{g}_1.\mathbf{u})}{\partial s_1}\right|_{\mathbf{r}_2} + \left.\frac{\partial(\mathbf{g}_2.\mathbf{u})}{\partial s_1}\right|_{\mathbf{r}_1} - \left.\frac{\partial(\mathbf{g}_2.\mathbf{u})}{\partial s_1}\right|_{\mathbf{r}_2}\right] \equiv B(s_0,s_2),\end{aligned} \tag{9}$$

where

$$\frac{\partial}{\partial s_1} = \frac{\mathbf{k}_0 + \mathbf{g}_1}{|\mathbf{k}_0|}\nabla \quad \text{and} \quad \frac{\partial}{\partial s_2} = \frac{\mathbf{k}_0 + \mathbf{g}_2}{|\mathbf{k}_0|}\nabla.$$

The solution of (9) can be written in the form

$$\Delta\mathbf{k}(p,s_0,s_2) = \frac{\mathbf{g}_1 \times \mathbf{g}_2}{|\mathbf{g}_1 \times \mathbf{g}_2|} p + \frac{A\mathbf{g}_2^2 - B\mathbf{g}_1.\mathbf{g}_2}{(\mathbf{g}_1 \times \mathbf{g}_2)^2}\mathbf{g}_1 + \frac{B\mathbf{g}_1^2 - A\mathbf{g}_1\mathbf{g}_2}{(\mathbf{g}_1 \times \mathbf{g}_2)^2}\mathbf{g}_2, \tag{10}$$

where the variables s_0 and s_2 lie in the ranges $(0, T/\cos\theta_1)$ and $[0, s_2^{\max}(s_0)]$, respectively. T is the thickness of the crystal and θ_1 is the Bragg angle. The coordinate $s_2^{\max}$ corresponds to the point $\mathbf{r}_2$, where a neutron with the wave vector $\mathbf{k}'(\mathbf{r}_1) + \mathbf{g}_2'(\mathbf{r}_1)$, reflected on the system of planes 2, leaves the crystal without tertiary reflection (see Fig. 1). As the coordinate s_2 is measured from the point $\mathbf{r}_1$, it is clear that $s_2^{\max}$ is a function of s_0. p is the free parameter dependent on the collimation of the incident beam and is independent of s_0 and s_2. It can be seen from (10) that this theoretical treatment is valid for sets of planes 1 and 2 for which $\mathbf{g}_1 \times \mathbf{g}_2 \neq 0$, *i.e.* planes 1 and 2 not parallel.

The intensity of the double reflected beam may be written in the form

$$I = \int N(\Delta\mathbf{k}).R(\Delta\mathbf{k})\,\mathrm{d}V, \tag{11}$$

where $N(\Delta\mathbf{k})$ is the density of incident neutrons with the wave vectors $\mathbf{k}_0 + \Delta\mathbf{k}$ related to the volume unit of reciprocal space and $R(\Delta\mathbf{k})$ is the 'common' reflectivity of both the second and third set of planes.

We assume in our model that $R(\Delta\mathbf{k})$ is equal to 1 if $\Delta\mathbf{k}$ fulfils (10) and to zero for other $\Delta\mathbf{k}$. The volume element $\mathrm{d}V$ can be expressed by the relation

$$\mathrm{d}V = \left| \left(\frac{\partial \Delta\mathbf{k}}{\partial s_0} \times \frac{\partial \Delta\mathbf{k}}{\partial s_2} \right) . \frac{\partial \Delta\mathbf{k}}{\partial p} \right| \times \mathrm{d}p\, \mathrm{d}s_0\, \mathrm{d}s_2 \quad (12)$$

$$= \frac{1}{|\mathbf{g}_1 \times \mathbf{g}_2|} \frac{\partial A(s_0)}{\partial s_0} \frac{\partial B(s_0, s_2)}{\partial s_2}\, \mathrm{d}p\, \mathrm{d}s_0\, \mathrm{d}s_2.$$

It is clear from (12) that only a deformation for which $\partial A/\partial s_0 \neq 0$ and $\partial B/\partial s_2 \neq 0$ are fulfilled simultaneously may excite the *Umweg* effect.

In the case of a vibrating single crystal, the displacement $\mathbf{u}$ can be generally expressed in the form

$$\mathbf{u}(\mathbf{r},t) = u_0 . f(\mathbf{r}) \sin \omega t, \quad (13)$$

where u_0 is the vibration amplitude and ω is the circular frequency. The form of the vector function $\mathbf{f}(\mathbf{r})$ depends on the vibration mode (Cady, 1946; Petržílka, Michalec, Chalupa, Sedláková, Mikula & Čech, 1975).

The above-mentioned lamellae model derived for the statistically slightly deformed crystal can be successfully used in the case of a vibrating one if the time which a neutron spends in the crystal is negligible in comparison with the vibration period. Otherwise, it is necessary for every moment (*e.g.* when the neutron enters the crystal) to replace the time-dependent displacement $\mathbf{u}(\mathbf{r},t)$ by a suitable static displacement $\mathbf{u}(\mathbf{r}) = \mathbf{u}[\mathbf{r}, t_0 + (s_0 + s_1 + s_2)/V_n]$, in which the time t_0 is used as a parameter (Michalec, Mikula & Vrána, 1975). The displacement $\mathbf{u}(\mathbf{r})$ relates to the deformation changes during the time which a neutron spends on the path through the crystal. Under these conditions, the problem of the vibrating crystal can be solved as a static one by the method derived above.

An analytic solution may simply be found if the displacement $\mathbf{u}(\mathbf{r})$ can be expressed with a good approximation in the quadratic form

$$u(\mathbf{r}) = u(0) + \sum_{i,j=0}^{2} \left(\left. \frac{\partial u}{\partial s_i} \right|_{\mathbf{r}=0} s_i + \frac{1}{2} \left. \frac{\partial^2 u}{\partial s_i\, \partial s_j} \right|_{\mathbf{r}=0} s_i s_j \right). \quad (14)$$

From the relations from (9) to (14) with the above assumptions, we can say that the intensity of the double reflected beam is time modulated approximately as the square of a sinusoidal function and proportionally to the square of the vibration amplitude u_0.

3. Experimental arrangement

The experiment was performed in the same experimental arrangement as was published in paper I. A beam of nearly monoenergetic neutrons with wavelength $\lambda = 1{\cdot}54 \times 10^{-1}$ nm impinged on the vibrating silicon bar set for the forbidden 222 diffraction in the position of the symmetric Laue transmission. We used two vibration modes in this experiment. The bar with dimensions 200 × 30 × 6 mm was excited into flexural vibrations with the resonance frequency $f = 1{\cdot}4$ kHz and the other bar with dimensions 110 × 14 × 3 mm was excited into longitudinal vibrations with the resonance frequency $f = 39$ kHz. The methods of the flexural and longitudinal excitation of crystal bars are well described in the papers of Petržílka, Vrzal, Michalec, Chalupa, Mikula & Zelenka (1970) and Mikula, Michalec & Vávra (1976), respectively. The elastic displacement $\mathbf{u}(\mathbf{r},t)$ took place in the $[1\bar{1}0]$ direction in the former case and in the [111] direction in the latter one.

For the azimuthal rotation we used the goniometer head which enabled the setting of Φ in the angle interval from −23 to +23°.

4. Experimental results

According to the paper of Cole, Chambers & Dunn (1962), we performed computer calculations of the azimuthal angle positions of the (222) planes in which other sets of planes might be operative in the wavelength band from $1{\cdot}52$ to $1{\cdot}56 \times 10^{-1}$ nm (see Fig. 2) corresponding to the $\Delta\lambda$ dispersion of the incident beam.

Fig. 3 shows the intensity–azimuth dependence for the case of the flexurally vibrating crystal bar. Curve (*a*) corresponds to the non-vibrating crystal and curve (*b*) to the vibrating one with vibration amplitude 30 μm. The width of the incident beam was 5 mm and the beam axis crossed the bar in the middle.

Fig. 4 presents the same azimuthal dependence for the case of the longitudinally vibrating crystal bar: curve (*a*) non-vibrating crystal and curve (*b*) vibrating one with amplitude 6 μm. The width of the incident

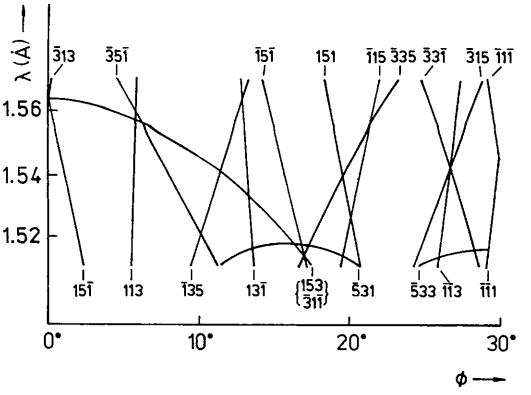

Fig. 2. The azimuth–wavelength relationship for the 222 reflection in the diamond structure of a Si crystal.

beam was 30 mm and its axis crossed the bar at 15 mm from the end. It means that in both cases the incident beam impinged on the bar at the place of maximum displacement **u**.

Fig. 5 experimentally depicts the result following from the approximative theory presented above, that in the region of the deformation, where the lamellae model can be used, the intensity of doubly diffracted neutrons, the so-called *Umweg* effect, is proportional to the square of the vibration amplitude. This amplitude dependence corresponds to the flexurally vibrating bar rotated to the azimuthal angle position $\Phi = 12{\cdot}01°$ where the maximum *Umweg* effect was observed.

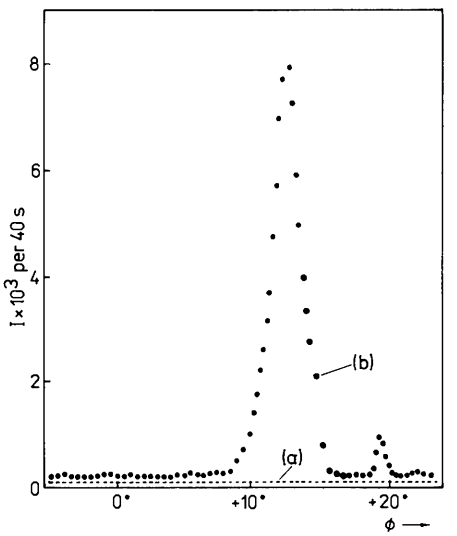

Fig. 3. The intensity–azimuth dependence for (*a*) the non-vibrating single crystal and (*b*) the flexurally vibrating crystal. The vibration amplitude was 30 μm.

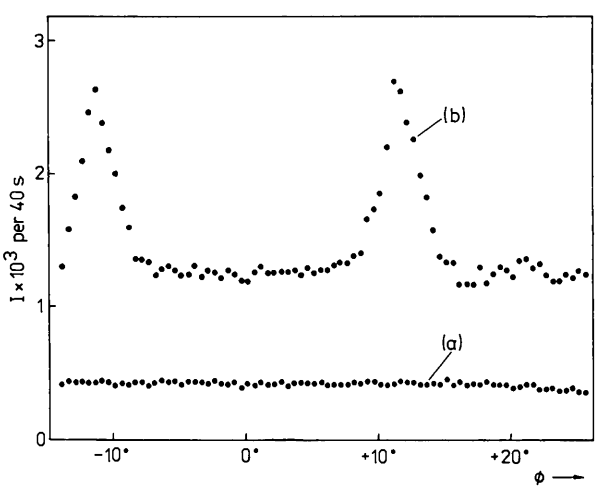

Fig. 4. The intensity–azimuth dependence for (*a*) the non-vibrating single crystal and (*b*) the longitudinally vibrating crystal. The vibration amplitude was 6 μm.

Fig. 6 illustrates the intensity of the allowed 111 reflection of the non-vibrating sample of dimensions 200 × 30 × 6 mm for $\Phi = 0°$, $\lambda = 1{\cdot}54 \times 10^{-1}$ nm and with incident beam width 5 mm.

5. Discussion

Fig. 2 shows that, for $\lambda = 1{\cdot}54 \times 10^{-1}$ nm, about 15 different secondary reflections may take part in multiple diffraction in the azimuthal angle interval Φ from 0 to

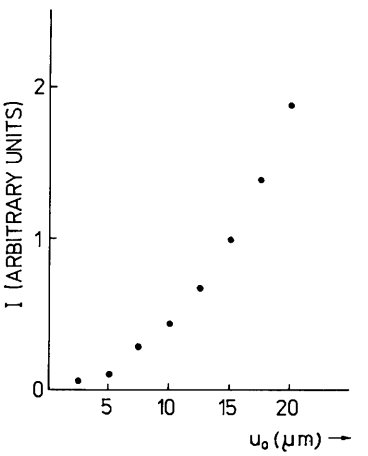

Fig. 5. The dependence of the intensity of doubly diffracted neutrons, corresponding to the *Umweg* effect at $\Phi = 12{\cdot}01°$, on the vibration amplitude u_0 of the flexurally vibrating crystal bar.

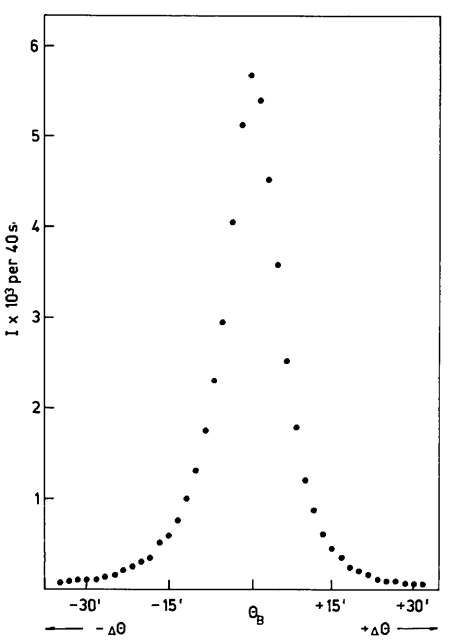

Fig. 6. Rocking curve obtained in the (111) diffraction setting of the non-vibrating crystal bar for $\Phi = 0°$ and $\lambda \simeq 1{\cdot}54 \times 10^{-1}$ nm.

30°. The experiment with the flexurally vibrating crystal demonstrates that the large *Umweg* effect takes place only at the angle $\Phi \simeq 12°$ (see Fig. 3). Further, we observed another effect at $\Phi \simeq 19{\cdot}5°$ which is about one order lower in comparison with the previous one.

For an explanation of these *Umweg* effects, we turn now to an evaluation of the intensity defined by (11). In our case of flexural vibrations, in the middle of the bar the deformation function $f(\mathbf{r})$ is well approximated by

$$f(\mathbf{r}) = \cos\left[\frac{\pi}{L}\left(\frac{\mathbf{g}_1}{|\mathbf{g}_1|}.\mathbf{r}\right)\right]$$

and $\nabla f(\mathbf{r})$ is parallel to $\mathbf{g}_1$.

After a simple calculation we obtain

$$I = G\frac{u_0^2.\pi^4}{4k^2L^4}\sin^2\omega t\int\frac{(\mathbf{g}_1.\mathbf{g}_2+\mathbf{g}_1.\mathbf{k})^2}{|\mathbf{g}_1\times\mathbf{g}_2|}\,dp\,ds_0\,ds_2, \quad (15)$$

where G is a constant and L is the length of the bar. The integration over p gives a constant. The limits of the integration over s_0 are 0 and $T|\mathbf{k}|/(\mathbf{k}.\mathbf{n})$, where $\mathbf{n}$ is the unit vector parallel to $[1\bar{1}0]$. The value of the coordinate s_2 is limited by the relations

$$\mathbf{r}_2.\mathbf{n} < T;\quad \frac{\mathbf{r}_2.\mathbf{g}_1}{|\mathbf{g}_1|} < \frac{L}{2};\quad \mathbf{r}_2.\mathbf{m} < \frac{P}{2}, \quad (16)$$

where T, L and P mean the thickness, length and height of the bar, respectively, and $\mathbf{m} = (\mathbf{n}\times\mathbf{g}_1)/|\mathbf{n}\times\mathbf{g}_1|$.

For an infinitely large crystal plate of thickness T ($P \to +\infty$; $L \to +\infty$), the contribution of the individual planes is given by

$$\begin{aligned} I' = {} & G'\sin^2\omega t\cos^2\alpha_{n2}\sin\theta_2 \\ & \times(2\sin\theta_2\cos\alpha_{12}-\sin\theta_1)^2 \\ & \times[\cos\Phi\sin 2\theta_1\sin^2\alpha_{12} \\ & \times(\cos\varphi\cos\theta_1+2\sin\theta_2\cos\alpha_{n2})]^{-1} \quad (17) \end{aligned}$$

where α_{12} and α_{n2} are the angles between the vectors $\mathbf{g}_1$ and $\mathbf{g}_2$ and $\mathbf{n}$ and $\mathbf{g}_2$. G' contains all the constants appearing during the integration in (15).

The results of the calculation in relative units are shown in Table 1. I' is the intensity calculated on the basis of (17) and I is the intensity corrected to the real dimensions of the flexurally vibrating bar.

It can be seen that only four secondary planes can substantially contribute to multiple diffraction in the azimuthal angle interval from 0 to 23° given by the experimental conditions. For these planes, the direction of s_2 is nearly perpendicular to $\mathbf{n}$ and so the diffracted beam on the secondary set of planes may have a relatively long path in the sample. The maximum intensity contributions come from the following secondary/tertiary reflections: $\bar{1}35/3\bar{1}\bar{3}$ at $\Phi = 11{\cdot}41°$, $153/13\bar{1}$ and $\bar{3}11/513$ at $\Phi = 12{\cdot}01°$ and $151/13\bar{1}$ at $\Phi = 19{\cdot}6°$. The comparison of the ratio of the peak intensities at $\Phi = 12{\cdot}01°$ and $\Phi = 19{\cdot}61°$ shows good agreement between the theoretical and experimental results. The zero contributions introduced in Table 1 follow from the special type of crystal deformation, *i.e.* $\mathbf{u}$ and $\nabla|\mathbf{u}|$ are parallel to $\mathbf{n}$ and $\mathbf{g}_1$, respectively.

Table 1. *Calculated intensities I' and I corresponding to an infinitely large crystal plate and to the crystal with dimensions used in the experiment, respectively, in relative units*

The sum of all contributions I' is taken to be 100%.

$\mathbf{g}_2$	Φ	I' (%)	I (%)
$[15\bar{1}]$	1·06	1·46	0·57
[113]	5·72	0	0
$[\bar{3}5\bar{1}]$	8·07	0·42	0·42
$[\bar{1}35]$	11·41	7·95	2·86
[153]	12·01	28·44	23·94
$[\bar{3}1\bar{1}]$	12·01	28·44	23·94
$[13\bar{1}]$	13·28	0	0
$[\bar{1}5\bar{1}]$	15·75	0	0
[151]	19·61	30·88	4·10
$[\bar{3}35]$	19·73	0·46	0·46
$[\bar{1}15]$	20·72	0·06	0·06
$[\bar{3}15]$	26·56	0	0
$[\bar{1}\bar{1}3]$	26·65	0	0
$[\bar{3}3\bar{1}]$	26·81	1·89	1·89
$[\bar{1}\bar{1}1]$	29·89	0	0

Because, independently of the type of deformation, the maximum effects give reflection planes for which the paths $s_2^{\max}$ are largest, it is clear that in the case of the longitudinal vibrations the largest *Umweg* effect was observed at the same azimuthal angle $\Phi = 12{\cdot}01°$, as in the case of the flexural vibrations (see Fig. 4).

The connection of the diffracted-intensity time modulation with the time-of-flight method made it possible to identify very simply the wavelength of the neutrons participating in simultaneous diffraction (see paper I). It was found that the *Umweg* peaks could be assigned to the neutrons of wavelength λ. On the other hand, the curves (*a*) in Figs. 3 and 4 can be assigned to the $\lambda/2$ neutrons. Comparing Figs. 3 and 4 (curves *b*), we can see that in the case of the longitudinal vibrations the 'background' to the *Umweg* effect is relatively high. This effect can be simply explained from the arrangement of the experiment. When the flexural vibrations are excited, the scalar product $\mathbf{g}_{444}.\mathbf{u}(\mathbf{r},t)$ is zero to a good approximation and the vibration has practically no effect on the $\lambda/2$ diffraction by the (444) planes. In the case of the longitudinal vibrations, $\mathbf{g}_{444}$ is parallel to $\mathbf{u}(\mathbf{r},t)$ and the vibration may have a significant influence on the intensity of the diffracted $\lambda/2$ neutrons (see paper I).

The very large effect observed at $\Phi = 12{\cdot}01°$ reveals that the elastic deformation can excite *Umweganregung* whose intensity is comparable to or even higher than the intensity corresponding to an allowed reflection (compare Figs. 3 and 6). As the density of the *Umweg*

peaks excited by an elastic deformation is much lower for $\lambda = 1{\cdot}54 \times 10^{-1}$ nm compared with $\lambda = 1{\cdot}05 \times 10^{-1}$ nm, the peaks can be experimentally eliminated by choosing a suitable azimuthal angle Φ.

The comparison of the experimental results with the theoretical ones in Table 1, as well as the proof of the quadratic intensity dependence on the vibration amplitude ($I \simeq u_0^2$), show that the developed lamellae model successfully explains the basic phenomena of multiple diffraction observed in an elastically deformed single crystal.

The authors wish to thank Miss B. Hašková and Mr A. Dvořák for their help in preparing the manuscript.

References

AZÁROFF, L. V., KAPLOW, R., KATO, N., WEISS, R. J., WILSON, A. J. C. & YOUNG, R. A. (1974). *X-ray Diffraction*. New York: McGraw-Hill.

BORMANN, G. & HARTWIG, W. (1965). *Z. Kristallogr.* **121**, 401–409.

BURAS, B., GIEBUŁTOWICZ, T., MINOR, W. & RAJCA, A. (1972). *Phys. Status Solidi A*, **9**, 423–433.

CADY, W. (1946). *Piezoelectricity*. New York: McGraw-Hill.

COLE, H., CHAMBERS, F. W. & DUNN, H. M. (1962). *Acta Cryst.* **15**, 138–144.

MICHALEC, R., CHALUPA, B., SEDLÁKOVÁ, L., MIKULA, P., PETRŽÍLKA, V. & ZELENKA, J. (1974). *J. Appl. Cryst.* **7**, 588–592.

MICHALEC, R., MIKULA, P. & VRÁNA, M. (1975). *Proceedings of the Fourth Conference of Czechoslovak Physicists, Liberec*. Prague: Academia.

MIKULA, P., MICHALEC, R. & VÁVRA, J. (1976). *Nucl. Instrum. Methods*, **137**, 23–27.

MIKULA, P., VRÁNA, M., MICHALEC, R. & VÁVRA, J. (1979). *Acta Cryst.* A**35**, 962–965.

MOON, R. M. & SHULL, C. G. (1964). *Acta Cryst.* **17**, 805–812.

PETRŽÍLKA, V., MICHALEC, R., CHALUPA, B., SEDLÁKOVÁ, L., MIKULA, P. & ČECH, J. (1975). *Nucl. Instrum. Methods*, **123**, 353–361.

PETRŽÍLKA, V., VRZAL, J., MICHALEC, R., CHALUPA, B., MIKULA, P. & ZELENKA, J. (1970). *Phys. Status Solidi*, **42**, 895–902.

RENNINGER, M. (1937). *Z. Phys.* **106**, 141–176.

TAKAGI, S. (1969). *J. Phys. Soc. Jpn*, **26**, 1239–1253.

THOMPSON, P. & GRIMES, N. W. (1977). *J. Appl. Cryst.* **10**, 369–371.

Acta Cryst. (1981). A**37**, 465–471

Thin-Crystal Approximations in Structure Imaging

BY P. PIROUZ*

Department of Metallurgy, Faculty of Engineering, University of Tehran, PO Box 1558, *Tehran, Iran*

(*Received* 28 *April* 1980; *accepted* 9 *January* 1981)

Abstract

Starting with the expression for the intensity distribution in a structure image, it is shown that, for a very thin crystal and constant value of the transfer function, there is a one-to-one correspondence between the image and the projection of potential distribution in the crystal along the beam direction. This is formally equivalent to the treatment of weak phase objects by Cowley & Iijima [*Z. Naturforsch. Teil A*, (1972), **27**, 445–451]. With a better approximation, applicable to slightly thicker crystals, it is shown that the image contrast is related not only to the projected potential distribution, but to the square of this function and the projected charge density. Simulated structure images of a silicon crystal, oriented with its [011] direction parallel to the incident beam, show that the distance between the closely spaced spots is increased along the [001] direction, in agreement with experimental images, which is a consequence of not enough diffracted beams contributing to the image as a result of spatial and temporal incoherence of the incident electron beam.

1. Introduction

Cowley & Iijima (1972) showed that, at the proper defocus, there is a direct correlation between the intensity distribution in a structure image of a very thin crystal and the projection of the crystal structure. Their analysis was based on the expansion of the transmission function of a phase object, which represents the change of phase of the electron wave on traversing the

* Presently at: Department of Metallurgy and Science of Materials, University of Oxford, Parks Road, Oxford OX1 3PH, England.

0567-7394/81/040465-07$01.00

© 1981 International Union of Crystallography